HHS Public Access

Author manuscript

Neuropharmacology. Author manuscript; available in PMC 2020 April 01.

Published in final edited form as:

Neuropharmacology. 2019 April ; 148: 320–331. doi:10.1016/j.neuropharm.2018.03.020.

N-Oleoyl-glycine reduces nicotine reward and withdrawal in mice

Giulia Donvito[a,1], **Fabiana Piscitelli**[b,1], **Pretal Muldoon**[a], **Asti Jackson**[a], **Rosa Maria Vitale**[b], **Enrico D'Aniello**[b,f], **Catia Giordano**[c], **Bogna M. Ignatowska-Jankowska**[a], **Mohammed A. Mustafa**[a], **Francesca Guida**[c], **Gavin N. Petrie**[d], **Linda Parker**[d], **Reem Smoum**[e], **Laura Sim-Selley**[a], **Sabatino Maione**[c], **Aron H. Lichtman**[a,g,*], **M. Imad Damaj**[a,**], **Vincenzo Di Marzo**[b,***], and **Raphael Mechoulam**[e]

[a]Department of Pharmacology and Toxicology, Medical College of Virginia Campus, Virginia Commonwealth University, Richmond, VA, USA

[b]Endocannabinoid Research Group, Institute of Biomolecular Chemistry, Consiglio Nazionale delle Ricerche, Pozzuoli, Naples, Italy

[c]Endocannabinoid Research Group, Department of Experimental Medicine, Section of Pharmacology, Second University of Naples, Naples, Italy

[d]Department of Psychology and Collaborative Neuroscience Graduate Program, University of Guelph, Guelph, ON, Canada

[e]Institute for Drug Research, Medical Faculty, Hebrew University, Jerusalem, Israel

[f]Department of Biology and Evolution of Marine Organisms, Stazione Zoologica Anton Dohrn, Naples, Italy

[g]Department of Medicinal Chemistry, Medical College of Virginia Campus, Virginia Commonwealth University, Richmond, VA, USA

Abstract

Cigarette smokers with brain damage involving the insular cortex display cessation of tobacco smoking, suggesting that this region may contribute to nicotine addiction. In the present study, we speculated that molecules in the insular cortex that are sensitive to experimental traumatic brain injury (TBI) in mice might provide leads to ameliorate nicotine addiction. Using targeted

[*]Corresponding author. Department of Pharmacology and Toxicology, Virginia Commonwealth University, PO Box 980613, Kontos Medical Sciences Building, 1217 East Marshall Street, Richmond, VA, 23298, USA. [**]Corresponding author. Department of Pharmacology and Toxicology, Virginia Commonwealth University, PO Box 980613, Kontos Medical Sciences Building, 1217 East Marshall Street, Richmond, VA, 23298, USA. [***]Corresponding author. Endocannabinoid Research Group, Institute of Bio-molecular Chemistry, Consiglio Nazionale delle Ricerche, Via Campi Flegrei 34, Comprensorio Olivetti, 80078, Pozzuoli, Napoli, Italy.

Authorship contributions

Participated in the research design: Donvito, Piscitelli, Petrie, Parker, Maione, Lichtman, Damaj, Di Marzo, Mechoulam.

Conducted experiments: Piscitelli, Muldoon, Jackson, Vitale, D'Aniello, Giordano, Guida, Ignatowska-Jankowska, Mustafa, Sim-Selley.

Contributed to reagents or analytical tool: Smoum.

Performed data analysis: Donvito, Piscitelli, Muldoon, Jackson, D'Aniello, Mustafa, Lichtman, Damaj, Di Marzo.

Wrote or contributed to the writing of the manuscript: Donvito, Piscitelli, Lichtman, Damaj, Di Marzo, Mechoulam.

[1]These authors contributed equally to this work.

Conflicts of interest

None.

Declarations of interest

Drs. Damaj, Di Marzo, Lichtman, Mechoulam, and Parker filed a provisional patent on oleoyl glycine.

lipidomics, we found that TBI elicited substantial increases of a largely uncharacterized lipid, *N*-acyl-glycine, *N*-oleoyl-glycine (OlGly), in the insular cortex of mice. We then evaluated whether intraperitoneal administration of OlGly would alter withdrawal responses in nicotine-dependent mice as well as the rewarding effects of nicotine, as assessed in the conditioned place preference paradigm (CPP). Systemic administration of OlGly reduced mecamylamine-precipitated withdrawal responses in nicotine-dependent mice and prevented nicotine CPP. However, OlGly did not affect morphine CPP, demonstrating a degree of selectivity. Our respective *in vitro* and *in vivo* observations that OlGly activated peroxisome proliferator-activated receptor alpha (PPAR-α) and the PPAR-α antagonist GW6471 prevented the OlGly-induced reduction of nicotine CPP in mice suggests that this lipid acts as a functional PPAR-α agonist to attenuate nicotine reward. These findings raise the possibility that the long chain fatty acid amide OlGly may possess efficacy in treating nicotine addiction.

Keywords

N-oleoyl glycine; Nicotine withdrawal; Cannabinoid receptor-1 (CB1); Conditioned place preference (CPP); Insular cortex; Peroxisome proliferator-activated receptor; alpha (PPAR-α)

1. Introduction

Dependence to tobacco represents one of the most frequent causes of mortality and morbidity in the world (Doll et al., 2004). Nicotine, a primary constituent of tobacco responsible for its rewarding effects, acts on nicotinic acetylcholine receptors (nAChRs), which are expressed on pre- and post-synaptic terminals (Albuquerque et al., 2009) in a variety of CNS pathways, including the mesolimbic reward system (Watkins et al., 2000). Chronic tobacco use often induces dependence and cessation can lead to affective (e.g., anxiety, anhedonia, depression, dysphoria, hyperalgesia, and irritability), somatic (e.g., tremors, bradycardia, gastrointestinal discomfort, and increased appetite), and cognitive (e.g., difficulty concentrating and impaired memory) withdrawal symptoms (Heishman et al., 2010). Naqvi and co-workers (Naqvi et al., 2007) reported that smokers with brain damage involving the insula, a region implicated in conscious urges, were more likely than smokers with brain damage not involving the insula to undergo a disruption of smoking addiction. Although the neurobio-logical mechanisms underlying this association remain to be determined, preclinical data also implicate a role of the insular cortex in nicotine reward. Specifically, rats given long access to nicotine self-administration had increased levels of dopamine and cAMP-regulated phosphoprotein of 32 kD phosphorylated at the protein kinase A site in the insular cortex (Abdolahi et al., 2010). This observation along with human data (Naqvi et al., 2014) suggest a role of this neuroanatomical region in addictive behavior and that neurochemicals within the insular cortex that are sensitive to brain injury may modulate nicotine addiction.

As a starting point to test molecules that may be useful to treat nicotine addiction, we sought to identify neurochemicals in the insular cortex of mice that may be altered by traumatic brain injury (TBI). Twenty-four h after TBI, we harvested insular cortex as well as comparison regions (i.e., hippocampus, and hypothalamus) for analysis. We initially focused

on endocannabinoids, because of their well-known involvement in nicotine reward and withdrawal signs in nicotine-dependent laboratory animals (Castañé et al., 2005, 2002; Gamaleddin et al., 2015; Le Foll and Goldberg, 2004; Merritt et al., 2008; Valjent et al., 2002), as well as related lipid signaling molecules. Among several investigated lipids, in addition to the endocannabinoids *N*-arachidonoylethanolamine (anandamide; AEA) (Devane et al., 1992) and 2-arachidonylglycerol (2-AG) (Mechoulam et al., 1995; Sugiura et al., 1995), we examined *N*-acylethanolamines, *N*-acyldopamines, *N*-acylserines and *N*-acylglycines.

Based on the results of the lipidomic analyses of TBI and control brain areas, we selected a largely uncharacterized member of the latter class, *N*-oleoyl glycine (OlGly) (Bradshaw et al., 2009). Specifically, we tested whether exogenous administration of this molecule would attenuate precipitated withdrawal responses in nicotine-dependent mice (Jackson et al., 2008). Additionally, we used the conditioned place preference paradigm (CPP) to infer whether it would attenuate the rewarding effects of nicotine (Kota et al., 2007). In order to elucidate potential underlying mechanisms of action of OlGly, we examined two likely targets. First, we tested whether it interacts with the endocannabinoid system. Specifically, we investigated if it binds to human recombinant CB_1 and CB_2 receptors transfected on HEK-293 cells, inhibits the primary AEA hydrolytic enzyme fatty acid amide hydrolase (FAAH), or elicits *in vivo* pharmacological effects, as assessed in the tetrad assay, which is highly sensitive to CB_1 receptor agonists (Little et al., 1988; Martin et al., 1991). Second, we examined whether it binds and produces its pharmacological effects through peroxisome proliferator-activated receptor α (PPAR-α), which has been demonstrated to play a role in nicotine dependence (Jackson et al., 2017; Mascia et al., 2011; Panlilio et al., 2012).

2. Material and methods

2.1. Subjects

Male ICR mice (6–8 weeks old; Harlan, Indianapolis, IN) with a body mass of 27–32 g served as subjects in all *in vivo* pharmacology experiments. Mice were group-housed (four per cage) for at least one week before the beginning of experiments on a 12/12 light/dark cycle (lights on at 0600 h), with an ambient temperature of 20–22 °C and humidity of 55–60%. Standard rodent chow and tap water were available ad libitum. Male C57BL/6 mice (Charles River, Italy) weighing 18–20 g were used for the mild TBI Weight Drop (WD) model.

All animal protocols were approved by the Virginia Commonwealth University Institutional Animal Care and Use Committee, were in accordance with the National Institutes of Health Guide for the Care and Use of Laboratory Animals and with the National Institutes of Health Guide for the Care and Use of Laboratory Animals, and by the Animal Ethics Committee of The Second University of Naples, in compliance with Italian (D.L. 116/92) and European Commission (O.J. of E.C. L358/1 18/12/86) regulations on the protection of laboratory animals.

2.2. Synthesis of OlGly

To a solution of oleic acid (1 gm, 3.54 mmol) and *N,N*-dime-thylformamide (266 μL, 3.64 mmol) in dry methylene chloride (10 mL) was added dropwise oxalyl chloride (2.0 M solution in methylene chloride, 3.5 mL, 7 mmol) under nitrogen atmosphere. The reaction mixture was stirred for 1 h and then the solvent was evaporated under a nitrogen flow. The crude material in methylene chloride (10 mL) was added to a solution of glycine (800 mg, 10.62 mmol) and 2 N potassium hydroxide in an ice bath. Then, the reaction mixture was stirred for 1 h, water (10 mL) was added, and the mixture was acidified to pH 3 with 1 N HCl. The product was extracted with ether (3 × 50 mL) and dried ($MgSO_4$), and solvent was evaporated under reduced pressure.

The crude material was chromatographed on silica gel (eluting with chloroform: methanol) to yield a crystalline solid. Melting point 93–94° C (degradation); LC-MS: $(M\text{-}H)^+$ 339 m/z; NMR (CD_3OH, ppm): 5.35–5.32 (m, 2H), 4.45 (s, 2H), 2.13–2.18 (m, 6H), 1.58 (m, 2H), 1.32–1.29 (m, 20H), 0.88 (t, 3H).

2.3. Drugs

$[^2H]_8$AEA, $[^2H]_5$2-AG, $[^2H]_4$ PEA, $[^2H]_4$ OEA, $[^2H]_8$ *N*-arachidonoyldopamine (NADA), $[^2H]_8$AraSer and $[^2H]_8$AraGly were purchased from Cayman Chemicals (MI, USA). OlGly was synthetized in the Mechoulam laboratory. The PPAR-α receptor antagonist GW6471 [N-((2S)-2-(((1Z)-1-methyl-3-oxo-3-(4-(trifluoromethyl)phenyl)prop-1-enyl)amino)-3-(4-(2-(5-methyl2phenyl-1,3-oxazol-4-yl) ethoxy)phenyl)propyl)propanamide] was purchased from tocris (Minneapolis, MN).

CP55,940 ((−)-cis-3-[2-hydroxy-4-(1,1-dimethylheptyl)phenyl]-trans-4-(3-hydroxypropyl)-cyclohexanol) and morphine sulfate were generously provided by NIDA (Rockville, MD). OlGly, CP55,940 and GW6471 were dissolved in a vehicle solution consisting of ethanol (5% of total volume), alkamuls-620 (Sanofi-Aventis, Bridgewater, NJ) (5% of total volume), and saline (0.9% NaCl) (90% of total volume). OlGly and CP55,940 were given via the intraperitoneal (i.p.) route of administration in a volume of 10 ml/kg (−)-Nicotine hydrogen tartrate [(−)-1-methyl-2-(3-pyridyl)pyrrolidine (+)-bitartrate] and mecamylamine HCl were purchased from Sigma-Aldrich Inc. (St. Louis, MO, USA). Morphine sulfate [morphine hemi[sulfate pentahydrate]] Nicotine and mecamylamine (2 mg/kg) were dissolved in physiological saline and given via the subcutaneous (s.c.) route of administration in a volume of 10 ml/kg. For the nicotine CPP study, 0.5 mg/kg nicotine dose was used because this dose reliably produces significant CPP in ICR mouse (Kota et al., 2007). Morphine CPP was performed with 10 mg/kg (s.c.) as recently described (Alajaji et al., 2016). For nicotine withdrawal studies, 24 mg/kg/day nicotine or saline was continuously perfused for 14 days using s.c. Osmotic minipumps (model 2002; Alzet Corporation, Cupertino, CA) that were implanted under isoflurane anesthesia. This prolonged nicotine administration regimen reliably produces significant withdrawal syndrome in the three behavioral paradigms used here (Jackson et al., 2009).

2.4. Surgical preparation and brain injury (mouse WD model)

Experimental mild TBI (TBI) was performed using a weight-drop device developed in the Naples laboratory. Mice were anesthetized with intraperitoneal injection of 250 mg/kg Avertin before being subjected to TBI. After a midline longitudinal incision, the skull was exposed to locate the area of impact and placed under a metal tube device where the opening was positioned directly over the animal's head. The injury was induced by dropping a cylindrical metal weight (50 g), through a vertical metal guide tube from a height of 20 cm. The point of impact was between the anterior coronal suture (bregma) and posterior coronal suture (lambda). Immediately following injury, the skin was closed with surgical wound clips and mice were placed back in their cages to allow for recovery from the anesthesia and TBI. Sham mice were submitted to the same procedure as described for TBI, but without release of the weight.

2.5. Extraction and quantification of endocannabinoids, N-acylethanolamines, N-acyldopamines, N-acylserines and N-acylglycines

Brain tissues were rapidly frozen, dounce-homogenized, and extracted with chloroform/methanol/Tris-HCl 50 mM pH 7.5 (2:1:1, v/v) containing internal deuterated standards for AEA, 2-AG, PEA, OEA, NADA, AraSer and AraGly quantification by isotope dilution (5 pmol for $[^2H]_8$AEA; 50 pmol for $[^2H]_5$2-AG, $[^2H]_4$ PEA and $[^2H]_4$ OEA; 10 pmol for $[^2H]_8$ NADA, $[^2H]_8$AraSer and $[^2H]_8$AraGly). Then the lipid extract was purified by open bed chromatography on silica. Fractions were eluted within increasing amounts of CH_3OH in $CHCl_3$ and part of the 9:1 (v/v) fraction was analyzed by liquid chromatography-atmospheric pressure chemical ionization-single quadrupole mass spectrometry for AEA, 2-AG, PEA and OEA levels, as previously described (Bisogno et al., 2009; Piscitelli et al., 2011). AEA, 2-AG, PEA and OEA levels were calculated on the basis of their area ratio with the internal deuterated standard signal areas. Part of the 9:1 fraction was used for *N*-acyldopamine identification, whereas the 7:3 fraction was used for *N*-acylglycine and *N*-acylserine identification and quantification by LC-MS-IT-TOF (Shimadzu Corporation, Kyoto, Japan) equipped with an ESI interface, using multiple reaction monitoring (MRM). The method for NADA was as previously described (Bisogno et al., 2009). Quantification was performed by isotope dilution by using m/z values of 370.3192 and 362.2692 corresponding to the molecular ion $[M+H]^+$ for deuterated and undeuterated AraGly; or *m/z* values of 400.3297 and 392.2795 corresponding to the molecular ion $[M+H]^+$ for deuterated and undeuterated AraSer The recovery of AraGly and AraSer from rat brain tissues using the extraction and analytical procedure reported here (see Methods) was 49.1 ± 15.7% and 42.1 ± 15.9% (n = 7). The LC-ESI-IT-ToF method was specific and exhibited a limit of detection (LOD, defined as the concentration at which the signal/noise ratio is greater than 3:1) of 50 fmol in the MS mode, and 1 pmol in the MS/MS mode for all the compounds analyzed. Moreover, the ratio between the $[M+H]^+$ peak areas of undeuterated (0.025–10 pmol) *vs.* deuterated (1 pmol) AraGly and AraSer varied linearly with the amount of the respective deuterated standards. The quantification limit of compounds was 100 fmol and the reproducibility of the method was 95%−99%. The chromatograms of the high-resolution $[M + H]^+$ values were extracted and used for calibration and quantification. LC analysis was performed in the isocratic mode using a Kinetex C18 Column (10 cm × 2.1 mm, 5 μm) and CH_3OH/water/acetic acid (85:15:0.1 by vol.) as the mobile phase with a flow rate of 0.15

ml/min. Identification of *N*-acyldopamines, *N*-acylglycines and *N*-acylserines was carried out using ESI ionization in the positive mode with nebulizing gas flow of 1.5 ml/min and curved desolvation line temperature of 250 °C.

2.6. Nicotine precipitated withdrawal studies

The minipumps were subcutaneously implanted in mice under isoflurane anesthesia. The pumps delivered 24 mg/kg/day nicotine or saline for 14 days. On the morning of day 15 (defined as 0 min), all mice that received nicotine were given an injection of OlGly (10, 30, or 60 mg/kg, i.p.) or vehicle (time: 0 min). At 15 min, each mouse was given an s.c. injection of the non-selective nicotinic acetylcholine receptor (nAChR) antagonist mecamylamine (2 mg/kg, s.c.). At 25 min, an experimenter, blinded to drug treatment, evaluated the mice in the elevated plus maze and then for physical (somatic) nicotine withdrawal signs, as previously described (Jackson et al., 2008). The mice were first evaluated for 5 min in the plus maze test in which the duration of time spent on the open arms versus closed arms of the plus maze was assessed. The number of arm crosses between the open and closed arms was also counted as a measure of locomotor activity. Immediately following plus maze assessment, each mouse was placed in a clear activity cage without bedding for a 20 min observation period of somatic signs measured that included paw and body tremors, head shakes, backing, jumps, curls, and ptosis. The total number of somatic signs was tallied for each mouse and the average number of somatic signs during the observation period was plotted for each test group. This testing sequence was chosen based on our prior studies showing that this order of testing reduced within-group variability and produced consistent results (Jackson et al., 2008). An observer blinded to experimental treatment performed all studies.

In order to test whether OlGly is brain penetrant, ICR mice received a single administration of OlGly (60 mg/kg, i.p.), or vehicle. After 15 min, plasma, insular cortex, hippocampus and hypothalamus were harvested and processed for the extraction and quanti-fication of the levels of OlGl,y as described above. The dose of OlGly used in this experiment and the time point for tissue collection were based on the behavioral experiments.

2.7. Conditioned place preference (CPP) studies

An unbiased CPP paradigm was performed, as previously described (Kota et al., 2007). Briefly, the CPP apparatus consisted of three chambers in a linear arrangement (MedAssociates, St. Albans, VT, ENV3013) with white and black chambers (20 × 20 × 20 cm each), which also differed in floor texture (white mesh or black rod). These chambers were separated by a small gray chamber with a smooth PVC floor. Partitions could be removed to allow access from the gray chamber to the black and white chambers. On day 1, animals were confined to the middle chamber for a 5-min habituation period and then allowed to move freely among all three chambers for 15 min. Time spent in each chamber was recorded, and no systematic bias was observed in baseline chamber preference. Twenty-min conditioning sessions occurred twice a day (days 2–4). During conditioning sessions, mice were confined to one of the larger chambers. The control group received saline in one large chamber in the morning and saline in the other large chamber in the afternoon. The nicotine group received nicotine in one large chamber and saline in the other large chamber.

Treatments were counterbalanced equally in order to ensure that some mice received nicotine in the morning while others received it in the afternoon. The nicotine-paired chamber was randomized among subjects. Sessions were 4 h apart and were conducted by the same investigator. On each of the conditioning days, mice were pretreated with OlGly (i.p.) or vehicle 15 min prior to nicotine or morphine (s.c.) injection. Five min after nicotine administration (0.5 mg/kg, s.c.), subjects were given 20-min conditioning sessions. In the morphine CPP comparison study, mice were given 30 min conditioning sessions following a 15 min pretreatment of morphine (10 mg/kg, s.c.) (Alajaji et al., 2016). In the PPAR-α antagonism study, GW6471 (2 mg/kg, i.p.) was injected 30 min before OlGly. On test day (day 5), mice were allowed access to all chambers for 15 min in a drug free state. The preference score was calculated by determining the difference between the time spent in the drug paired side during test day versus the time in drug paired side during the baseline day.

2.8. Tetrad behavioral assessment

Mice were acclimated to the test environment for at least 1 h prior to testing for tetrad components: spontaneous activity, catalepsy, antinociception, and hypothermia (Little et al., 1988; Martin et al., 1991; Wiley and Martin, 2003). Mice were assessed for baseline tail withdrawal latencies and body temperature, given an intraperitoneal (i.p.) injection of vehicle or drug (OlGly), and 30 min later assessed in the following order: catalepsy, tail withdrawal test, and body temperature.

In the locomotor studies, subjects were administered vehicle or drug and 5 min later were placed into clear acrylic boxes (approx. 44.5 cm × 22.25 cm × 20.0 cm) contained within sound-attenuating cabinets equipped with an LED light source and fans for general air circulation and creation of white noise. The distance traveled was expressed in cm and the time spent immobile in s collected and recorded for 10 min using Fire-i™ digital cameras purchased from Unibrain (San Ramon, CA, USA) and ANY-maze™ video tracking software purchased from Stoelting Company (Wood Dale, IL, USA). Catalepsy was assessed in the bar test, and the dependent measure was expressed as immobility time during a 60 s observation period (Ignatowska-Jankowska et al., 2015). Anti-nociception data were transformed to represent a maximum percent effect (%MPE) by the following formula: %MPE = [(test latency−pretreatment latency)/(10−pretreatment latency)] × 100. Body temperature data were expressed as a difference between the values collected before ad after the drug or vehicle administration (Δ temperature, °C).

2.9. Cumulative CP55,940 dose-response study

This experiment examined whether OlGly would shift the cumulative dose-response curves of CP55,940 in producing catalepsy, antinociception, and catalepsy, an *in vivo* assay sensitive to CB_1 receptor allosteric modulators (Ignatowska-Jankowska et al., 2015). Mice were pretreated with either OlGly (60 mg/kg i.p.) or vehicle 10 min before they received the first dose of CP55,940 followed by each subsequent dose every 40 min. Measurements for catalepsy, in (bar test), tail-flick, and rectal temperature were taken 30 min following each CP55,940 administration, as well as prior to any injections to determine baseline responses. Cumulative doses of CP55,940 were 0.3, 1, and 3 mg/kg i.p. Locomotor activity was not assessed due to habituation effects that occur following repeated testing.

2.10. Cannabinoid receptor binding

Membranes from HEK-293 cells stably transfected with the human recombinant CB_1 receptor (B_{max} = 2.5 pmol/mg protein) and human recombinant CB_2 receptor (B_{max} = 4.7 pmol/mg protein) were incubated with [^{3}H]-CP-55,940 (0.14 nM/kd = 0.18 nM and 0.084 nM/kd = 0.31 nM respectively for CB_1 and CB_2 receptor) as the high affinity ligand and displaced with 10 μM WIN 55212–2 as the heterologous competitor for nonspecific binding (K_i values: 9.2 nM and 2.1 nM respectively for CB_1 and CB_2 receptor). OlGly was tested following the procedure described by the manufacturer (Perkin Elmer, Italia). Displacement curves were generated by incubating drugs with [^{3}H]-CP-55,940 for 90 min at 30 °C. OlGly effect on AEA hydrolysis by rat brain membranes, which express high levels of fatty acid amide hydrolase, were assayed as previously described (Ortar et al., 2007).

2.11. Molecular modelling studies on OlGly

Starting ligand geometry was built with Ghemical 2.99.2 (Hassinen and Peräkylä, 2001), followed by energy minimization (EM) at molecular mechanics level first, using Tripos 5.2 force field parametrization, and then at AM1 semi-empirical level. OlGly was fully optimized using GAMESS program at the Hartree-Fock level with STO-3G basis set to derive the partial atomic charges using the RESP procedure of restrained fit to the HF/6–31G*/STO-3G electro-static potential. Docking studies were performed with AutoDock 4.2 (Morris et al., 2009). The crystallographic structure of PPAR-α (PDB entry 2P54) and the ligand were processed with AutoDock Tools (ADT) package version 1.5.6rc1 (Morris et al., 2009) to merge non polar hydrogens, calculate Gasteiger charges and select rotatable side-chain bonds. Grid for docking evaluation with a spacing of 0.375 Å and 50 × 50 × 70 points, centered in the ligand binding pocket, was generated using the program AutoGrid 4.2 included in Autodock 4.2 distribution. A 100 molecular docking run was performed adopting a Lamarckian Genetic Algorithm (LGA) and the following associated parameters: 100 individuals in a population with a maximum of 15 million energy evaluations and a maximum of 37000 generations, followed by 300 iterations of Solis and Wets local search. The docking results was subjected to visual inspection and as representative binding pose was selected the one with most favorable binding energy for the subsequent MD simulations of ligand-PPAR-α complex. The complex was completed by addition of all hydrogen atoms and underwent EM and then MD simulations with Amber12 pmemd.cuda module (Götz et al., 2012), using ff12SB version of AMBER force field (Case et al., 2012) for the protein and gaff parameters for the ligand.

To perform molecular dynamics (MD) simulation in solvent, the complex was confined in TIP3P water periodic box exhibiting a minimum distance between solute and box surfaces of 10 Å, using the tleap module of AmberTools12 program (Wang et al., 2004). The system was then neutralized by addition of counterions (Na+) and underwent 1000 steps of EM with solute atoms harmonically restrained to their starting positions using a force constant of 10 kcal mol-1Å-1. The solvated complex was submitted to 90 ps restrained MD (5 kcal mol-1Å-1) at constant volume, gradually heating the system to 300 K, followed by 60 ps restrained MD (5 kcal mol-1Å-1) at constant temperature (300 K) and pressure (1 atm) to adjust system density. Production MD simulation was carried out at constant temperature

(300 K) and pressure (1 atm) for 50 ns with a time-step of 2 fs. Bonds involving hydrogens were constrained using the SHAKE algorithm (Ryckaert et al., 1977).

2.12. PPAR-α luciferase assays

COS-7 cells (monkey kidney fibroblast-like cells) were grown in DMEM supplemented with 10% fetal bovine serum and 1% Pen/Strep under standard conditions. Cells were plated in a 24-well plate at confluence and transfected using Lipofectamine LTX and PLUS Reagent (Life Technologies 15338–100) according to the manufacture's instruction. At day 1, for each well, a combination of 25 ng of mouse PSG5- PPAR-α (plasmid 22751; Addgene), 300 ng of PPRE X3-TK-luc; (Plasmid 1015 Addgene), 100 ng of pSV-β-Galactosidase Control Vector (Promega E1081) and 75 ng pcDNA3 (Invitrogen) empty vector to a total of 500 ng were transfected. The following day, the growth media was replaced with fresh media containing compounds listed below and treated overnight. Ethanol was used as vehicle. At day 3 after 18 h of treatment cells were harvested and processed for the Luciferase and β -Galactosidase detection analysis.

Luciferase Gene Reporter activity was detected using the Luciferase kit (Sigma, LUC1) whereas β-Galactosidase Activity was detected with the β-Galactosidase detection kit (Sigma, Gal-A). β-Galactosidase expression was quantified with the Microplate Readers (Tecan) and used as an internal experimental control to analyze the transfection efficiencies in each cell sample group. The levels of Firefly Luciferase chemiluminescence intensity was detected with a ChemiDoc MP system station using the Imagelab software (Biorad) and reported normalized with respect to the β-Gal expression.

2.13. Statistical analysis

Lipid levels are expressed as means ± SEM of pmols/g wet tissue weight, unless otherwise stated. One-way ANOVA followed by the Tukey's test was used for comparisons of AEA, 2-AG, PEA, OEA and OlGly levels among the various groups. Unpaired t-test was used to analyze the data on the distribution of OlGly in the brain.

In the nicotine withdrawal studies, the data were analyzed by two-way ANOVA followed by Holm-Sidak's post-hoc test. For conditioned place studies, a preference score was calculated by subtracting time spent in the nicotine-paired chamber postconditioning minus the time spent pre-conditioning. A positive value indicated a preference for the nicotine- (or morphine-) paired compartment, whereas a negative value indicated an avoidance of the nicotine- (or morphine-) paired compartment. A number at or near zero indicated no preference. Data were analyzed by one-way ANOVA and further analyzed by the Student Neuman-Keuls post-hoc test.

In tetrad studies and luciferase assay, data were analyzed by one-way ANOVA followed by the Dunnett's post-hoc test. In the cumulative dose-response of CP55,940, data were analyzed by two-way ANOVA followed by the Sidak post-hoc test. In the luciferase assay, the Student's t-test with Welch's correction was applied. In the binding studies, K_i values were calculated by applying the Cheng-Prusoff equation to the IC_{50} values for the displacement of the bound radioligand by increasing concentrations of the test compound. Data are expressed as means ± SEM of at least n 3 = experiments.

The computer program GraphPad Prism version 6.0 (GraphPad Software Inc., San Diego, CA) was used in all statistical analyses. All data are expressed as mean ± SEM. A P value of <0.05 was considered statistically significant.

3. Results

3.1. OlGly levels are increased in the insular cortex of TBI mice

Experimental TBI increased OlGly levels, but not other analyzed lipids, in the insular cortex of mice [$F(2,10) = 15.46$, $p < 0.001$; Fig. 1A] compared to sham and naïve mice. However, OlGly levels did not significantly differ between brain-injured and sham groups in the hippocampus (Fig. 1B) or hypothalamus (Fig. 1C), indicating regional selectivity. The chromatograms show the presence of OlGly in the insula of TBI mice (Fig. 1D), but not in sham (Fig. 1E) or naïve (Fig. 1F) mice. Fig. 2 shows endocannabinoid levels (i.e., AEA, 2-AG) and related *N*-acyl-ethanolamines levels (i.e., PEA, OEA) in each of the three brain regions. As shown in Fig. 2A, TBI elicited a significant decrease in AEA levels in the insula [$F(2,8) = 19.18$, $p < 0.001$] and hippocampus [$F(2,8) = 7.587$, $p < 0.01$]. The levels of other investigated fatty acid amides in the examined brain regions of each experimental group were below detection.

3.2. OlGly attenuates nicotine withdrawal and nicotine reward

Based on the mouse brain injury data revealing a region-selective increase of OlGly in the insula, we elected to examine whether an i.p. injection of OlGly given 15 min before the nicotine receptor antagonist mecamylamine would prevent withdrawal signs in nicotine-dependent mice. Whereas nicotine-dependent mice undergoing precipitated withdrawal showed a decrease of time spent exploring the open arm in the elevated plus maze assay, OlGly (30 and 60 mg/kg, i.p.) significantly increased open arm time [$F(3, 56) = 4.661$, $p < 0.01$; Fig. 3A]. Moreover, 60 mg/kg OlGly attenuated the number of mecamylamine-precipitated somatic withdrawal signs in nicotine-dependent mice [$F(3, 56) = 3.439$, $p < 0.01$; Fig. 3B], but did not elicit overt behavioral alterations in control mice continuously infused with saline.

Next, we evaluated whether i.p. administration of the most effective dose of OlGly (60 mg/kg) is brain penetrant. Fifteen minutes following the injection, we detected OlGly levels in plasma (2004 ± 626.9 pmol/ml), insula (168.0 ± 60.28 pmol/g), hippocampus (186.0 ± 60.05 pmol/g), and hypothalamus (245.6 ± 108.1 pmol/g). In contrast, OlGly levels were below the limit of quantification in the vehicle-injected group.

3.3. OlGly attenuates nicotine-induced CPP

We employed the CPP assay, in order to test whether OlGly reduces the rewarding effects of nicotine. OlGly dose-dependently prevented the development of nicotine-induced CPP [$F(7,55) = 12.77$, $p < 0.001$; Fig. 4A], but did not affect place preference in saline-treated mice. However, the OlGly reduction of nicotine CPP did not carry over to morphine CPP (Fig. 4B), suggesting that OlGly is comparatively selective in blocking nicotine CPP.

3.4. OlGly does not functionally interact with the endogenous cannabinoid system

Because the endogenous cannabinoid system modulates numerous indices of nicotine reward and dependence, the next series of experiments investigated OlGly in a variety of *in vivo* and *in vitro* assays indicative of cannabimimetic activity. OlGly (10, 30, and 100 mg/kg i.p.) did not elicit significant effects in the tetrad assay, a battery of *in vivo* measures highly associated with CB_1 receptor activity (Martin et al., 1991). Specifically, OlGly did not elicit catalepsy in the bar test, antinociceptive effects in the tail-flick test, hypothermia, or hypomotility (Table 1). Additionally, OlGly did not alter the dose-response relationship of the high efficacy CB_1 receptor agonist CP55,940 (Devane et al., 1988) in the tetrad assay (Fig. 5), suggesting that it does not act functionally as a CB_1 receptor antagonist or CB_1 receptor allosteric modulator. Finally, OlGly did not bind CB_1 or CB_2 receptors and weakly inhibited FAAH (Table 2).

3.5. OlGly elicits its effects via PPAR-α mechanism of action

Considering that OlGly possesses a chemical structure similar to OEA, which acts as an endogenous PPAR-α ligand, we next assessed whether OlGly binds PPAR-α as well as produces functional activity at this receptor. As shown in the modeling experiment, OlGly binds PPAR-α (Fig. 6A), and behaved as a PPAR-α receptor agonist in a specific luciferase assay for functional activity (Fig. 6B). The selective PPAR-α agonist GW7647 (comparison drug), as well as OlGly, significantly increased luciferase activity compared to DMSO [$F(5,44) = 17.7$, $p < 0.0001$].

Given this *in vitro* evidence suggesting that OlGly behaves as a PPAR-α receptor agonist, we next examined whether PPAR-α mediates OlGly prevention of nicotine CPP. As shown in Fig. 6C, the selective PPAR-α antagonist GW6471 fully prevented OlGly blockade of nicotine CPP [$F(6, 56) = 12.8$, $p < 0.0001$].

4. Discussion

The impetus of the present study was based on a report that nicotine addiction was ameliorated in cigarette smokers suffering from brain damage that included the insular cortex compared with brain-damaged individuals that did not involve the insula, suggesting that this brain region may play an important role in smoking addiction (Naqvi et al., 2014, 2007). We speculated that experimental brain injury in mice might alter neurochemicals in this brain region that may serve as a starting point for identifying new molecules to treat nicotine addiction. Accordingly, we examined the lipidomic profile of the insular cortex in mice subjected to TBI and found a profound increase of a largely uncharacterized *N*-acylglycine, OlGly, in the insular cortex, but not in hippocampus or hypothalamus. *N*-acylglycines represent a possible class of endogenous signaling molecules, which are structurally related to endocannabinoids, and have recently generated research interest due to their remarkable biological activities, such as anti-inflammatory effects (Burstein et al., 2011), inhibition of cancer cell proliferation (Chatzakos et al., 2012), adipogenesis (Wang et al., 2015), and neural protection (Cohen-Yeshurun et al., 2011). Based on this regionally selective increase of OlGly, we sought to test whether its exogenous administration would ameliorate withdrawal-associated behaviors in nicotine-dependent mice as well prevent

nicotine reward in the mouse CPP model. Three general findings support the idea that OlGly may serve to counteract nicotine addiction. First, OlGly reduced somatic withdrawal signs as well as affective behavior in nicotine-dependent mice undergoing precipitated withdrawal. Second, OlGly prevented the development of nicotine CPP. Third, a singular systemic administration of the most effective dose of OlGly in naïve mice results in an increase of OlGly contents within plasma, and in the brain to levels similar to those found in mice after TBI.

Few studies have investigated the pharmacological effects of OlGly. Although it has been detected in different tissues, including rat spinal cord, brain, lung, skin, ovaries, liver, spleen, and kidney (Bradshaw et al., 2009), the present study is the first to quantify it in specific brain regions. OlGly biosynthesis results from a reaction between oleoyl CoA and glycine, which can be catalysed by either glycine *N*-acyltransferase-like 3, or cytochrome c in the presence of hydrogen peroxide (Wang et al., 2015), while FAAH participates in its degradation (Bradshaw et al., 2009). Additionally, OlGly may play a role in the biosynthesis of oleamide, another substrate of FAAH that mediates several fundamental neurochemical processes (Boger et al., 1998) including sleep (Huitron-Resendiz et al., 2004), thermoregulation, and nociception (Fedorova et al., 2001). OlGly and oleamide possess equal potency in eliciting hypothermia and decreasing locomotion in rats. However, the failure of OlGly to increase circulating levels of oleamide suggests that its pharmacological effects occur independently of its conversion to oleamide. In addition to its structural similarity to the *N*-acylethanolamines, which include AEA, as well as PPAR-α agonists OEA and palmitoylethanolamide (PEA), recent evidence suggests that OlGly may play a role in enhancing insulin sensitivity through a CB_1 receptor mechanism of action (Wang et al., 2015). The CB_1 receptor also plays an important role in mediating the rewarding effects of nicotine. For example, a CB_1 receptor antagonist administered either systemically or into the ventral tegmental area (VTA) decreased nicotine self-administration in rats (Le Foll and Goldberg, 2004; Simonnet et al., 2013). Similarly, CB_1 (−/−) mice or wild type animals treated with a selective CB_1 receptor antagonist do not display nicotine CPP (Castañé et al., 2002; Le Foll and Goldberg, 2004; Merritt et al., 2008), indicating that this receptor plays a necessary role in multiple laboratory models of nicotine reward. Likewise, genetic deletion or pharmacological inhibition of CB_2 receptors blocks nicotine reward-like effects in the nicotine self-administration and nicotine CPP paradigms in mice (Ignatowska-Jankowska et al., 2013; Navarrete et al., 2013). In contrast, a CB_2 receptor antagonist did not affect either nicotine self-administration or reinstatement of nicotine seeking in rats (Gamaleddin et al., 2012). These divergent results of the effectiveness of CB_2 receptor antagonists in reducing nicotine reward may be related to species differences. Importantly, clinical trials revealed the CB_1 receptor antagonist rimonabant effectively improved smoking abstinence compared with placebo, though clinical development of this and other CB_1 receptor antagonists was terminated due to unacceptable adverse effects (Robinson et al., 2017). The question of whether a CB_2 receptor antagonist has efficacy in treating smoking addiction remains to be determined.

Based on the extensive role that the endogenous cannabinoid system plays on nicotine reward, we tested whether OlGly interacts with this system. OlGly did not produce *in vivo* pharmacological activity indicative of CB_1 receptor stimulation as assessed in the tetrad

assay, consisting of catalepsy, antinociception, hypothermia, and hypomotility measures (Little et al., 1988; Martin et al., 1991; Wiley and Martin, 2003). In contrast, Chaturvedi and colleagues reported that OlGly reduces body temperature (1.5–2.0 °C) and decreases locomotor activity in rats (Chaturvedi et al., 2006). The disparate results between their finds and the results in the present study may be a consequence of species differences or other methodological considerations (e.g., housing of the animals, ambient room temperature, etc.). At any rate, the previous study did not examine CB_1 receptor involvement of the hypothermic or decreases locomotor activity effects of OlGly. Furthermore, the fact that OlGly poorly binds human recombinant CB_1 and CB_2 receptors suggests direct action at these receptors is unlikely. Another possibility is that OlGly behaves as an allosteric modulator of the CB_1 receptor. Accordingly, we examined whether OlGly would alter the antinociceptive, cataleptic, and hypothermic effects of the high efficacy, orthosteric CB_1 receptor agonist CP55,940. Whereas the CB_1 receptor positive allosteric modulator ZCZ011 elicited a leftward shift of the CP55,940 dose-response curve for each of these measures (Ignatowska-Jankowska et al., 2015), OlGly did not affect the CP55,940 dose-response curves. It is noteworthy that FAAH inhibitors reduce nicotine self-administration and nicotine priming-induced reinstatement through PPAR-α in squirrel monkeys, consistent with the idea that the endogenous substrates of this enzyme counteract nicotine reward by activating this nuclear receptor (Justinova et al., 2015). In contrast, Forget and colleagues have found that inhibition of FAAH reduced nicotine reinstatement, but did not affect nicotine self-administration (Forget et al., 2009). Accordingly, our experiment showing that OlGly only weakly inhibits AEA hydrolysis suggests the unlikelihood of indirect activation of cannabinoid receptors or other AEA targets through FAAH inhibition.

Structural similarities between OlGly and OEA, which activates PPAR-α, raise the possibility that OlGly may likewise prevent the development of nicotine CPP through this receptor. Notably, PPAR-α has been implicated in the control of nicotine reward (Jackson et al., 2017; Mascia et al., 2011; Panlilio et al., 2012). The modeling experiment presented here revealing that OlGly binds PPAR-α and the finding that OlGly behaved as a PPAR-α agonist in a specific luciferase assay support this hypothesis. Another noteworthy finding in the present study is that the selective PPAR-α antagonist GW6471 fully prevented OlGly blockade of nicotine CPP, indicating that this anti-reward effect of OlGly requires PPAR-α receptor activation. These results are consistent with recent reports on PPAR-α agonists blocking nicotine withdrawal, nicotine CPP, nicotine self-administration, and nicotine priming-induced reinstatement in rodents and nonhuman primates (Jackson et al., 2017; Mascia et al., 2011; Panlilio et al., 2012). However, fenofibrate, a low efficacy and non-selective PPAR-α agonist, did not facilitate the ability to stop smoking during a brief practice quit period in dependent smokers (Perkins et al., 2016). In addition, it failed to reverse nicotine withdrawal in mice (Jackson et al., 2017). Nonetheless, clinical studies employing PPAR-α agonists with higher efficacy and selectivity remain to be conducted.

The findings that OlGly dose-dependently reduced the development of nicotine-induced CPP, but did not affect morphine CPP, suggest selectivity for blocking nicotine CPP. This observation is consistent with work reviewed by Melis and Pistis (2014), who reported that the “anti-addictive” properties of PPAR-α stimulation show selectivity for reducing nicotine reward over the reinforcing effects of cocaine, cannabinoids, and morphine (Melis and

Pistis, 2014). A parsimonious explanation accounting for the selectivity of OlGly in blocking nicotine CPP includes a complex neurochemical pathway involving PPAR-α activity inducing negative modulation of β2*-nAChR receptor activity expressed on VTA dopamine cells that ultimately dampen nicotine-induced firing and bursting activity (Melis et al., 2013). Similarly, fenofibrate induced a reduction of stress-induced depression behaviors in mice through phasic activation of the mesolimbic dopaminergic system (Scheggi et al., 2016). Additionally, it has been reported that local infusion of dopamine receptor 1 antagonist into the insular cortex significantly decreased nicotine self-administration in rats (Kutlu et al., 2013).

According to the model proposed by Naqvi and Bechera, the insula belongs to a network, which includes the ventromedial prefrontal cortex, anterior cingulate cortex, NAc, and amygdala, responsible for the conscious pleasure from drugs, drug craving, drug seeking behavior, and drug relapse. Specifically, the insula processes interoceptive information about the drugs received from a thalamocortical pathway and relays this information to the pre-frontal regions and the amygdala, which evoke pleasure related effects of the drugs through dopaminergic activation in the VTA (Naqvi and Bechara, 2010). According to their model, the insula serves as a critical neural substrate for addiction by regulating the dopaminergic signal in the VTA. However, whether a direct connection exists between the mesolimbic dopamine system and PPAR-α–induced reduction of nicotine CPP by OlGly remains an unanswered question. It will also be important to determine whether the anti-nicotine CPP effects of OlGly extend to self-administration and reinstatement procedures.

We based the rationale to investigate the effects of OlGly on nicotine CPP and withdrawal responses in nicotine-dependent mice from lipidomic analyses of the insular cortex from mice following TBI. Although the present study does not address the neural substrates underlying these effects, we found that following a singular i.p. administration of a dose of OlGly that was most effective in reducing nicotine withdrawal, the levels of OlGly increased within the insula, hippocampus, hypothalamus and plasma up to concentrations that were similar to those detected after TBI. Nonetheless, other preclinical research supports a role of the insular cortex on nicotine reward. Whereas inactivation of insula by local infusion of γ–aminobutyric acid agonist mixture decreased nicotine self-administration in rats (Forget et al., 2010; Pushparaj et al., 2015), electrical stimulation of this region significantly attenuated nicotine reinforcement as well as nicotine-seeking behaviors. These findings suggest that the insular cortex may play a modulatory role in nicotine reward (Pushparaj et al., 2013). In the case of dependence, both central and peripheral nicotinic receptors mediate somatic nicotine withdrawal signs, while central nicotinic receptor populations, such as the nucleus accumbens (NAc) and habenulo-interpeduncular system regulate anhedonia, anxiety, and aversion (De Biasi and Dani, 2011; Watkins et al., 2000). Furthermore, the mesohabenular pathway through the interpeduncular nucleus and corticotropin-releasing factor-1 (CRF1) receptors in the central nucleus of the amygdala (CeA) seem to play a preponderant role in the emergence of anxiety-like behaviors in nicotine-dependent animals (Cohen et al., 2015). Thus, the neural sites of action of OlGly and whether the elevated levels of OlGly in the insular cortex produced by TBI ameliorates nicotine reward and/or dependence remain to be determined.

5. Conclusions

The present study demonstrates an alteration in the lipid profile in the insular cortex compared to other neural regions of mice subjected to TBI. In particular, we found a significant increase of OlGly levels in the insula, a region implicated in smoking addiction (Naqvi et al., 2014, 2007). A potential PPAR-α mechanism of action is consistent with several reports showing that PPAR-α agonists attenuate nicotine reinforcement and reinstatement in rodents and nonhuman primates (Mascia et al., 2011; Panlilio et al., 2012), though the neuroanatomical substrates remain to be determined as well as the potential translational efficacy in humans. Nonetheless, the findings that i.p. administration of OlGly prevented both nicotine CPP and nicotine withdrawal-associated behaviors in mice, and that the injection of the same effective dose of OlGly in naïve mice was brain penetrant suggest that this ligand may be of value in treating addiction to tobacco smoking in humans.

Funding

This work was supported by NIH grants P01DA009789, R01DA039942, P30DA033934 (AHL); R01 DA032246 and P50DA039841 (MID), T32DA007027 (AJ), and startup funds from the VCU School of Pharmacy. NSERC (92056) and CIHR (137122) grants to LAP.

References

Abdolahi A, Acosta G, Breslin FJ, Hemby SE, Lynch WJ, 2010 Incubation of nicotine seeking is associated with enhanced protein kinase A-regulated signaling of dopamine- and cAMP-regulated phosphoprotein of 32 kDa in the insular cortex. Eur. J. Neurosci 31, 733–741. 10.1111/j.1460-9568.2010.07114.x. [PubMed: 20384816]

Alajaji M, Lazenka MF, Kota D, Wise LE, Younis RM, Carroll FI, Levine A, Selley DE, Sim-Selley LJ, Damaj MI, 2016 Early adolescent nicotine exposure affects later-life cocaine reward in mice. Neuropharmacology 105, 308–317. 10.1016/j.neuropharm.2016.01.032. [PubMed: 26808314]

Albuquerque EX, Pereira EFR, Alkondon M, Rogers SW, 2009 Mammalian nicotinic acetylcholine receptors: from structure to function. Physiol. Rev 89, 73–120. 10.1152/physrev.00015.2008. [PubMed: 19126755]

Bisogno T, Piscitelli F, Di Marzo V, 2009 Lipidomic methodologies applicable to the study of endocannabinoids and related compounds: Endocannabinoidomics. Eur. J. Lipid Sci. Technol 111, 53–63. 10.1002/ejlt.200800233.

Boger DL, Patterson JE, Guan X, Cravatt BF, Lerner RA, Gilula NB, 1998 Chemical requirements for inhibition of gap junction communication by the biologically active lipid oleamide. Proc. Natl. Acad. Sci. U. S. A 95, 4810–4815. [PubMed: 9560184]

Bradshaw HB, Rimmerman N, Hu SS-J, Burstein S, Walker JM, 2009 Novel endogenous N-acyl glycines identification and characterization. Vitam. Horm 81, 191–205. 10.1016/S0083-6729(09)81008-X. [PubMed: 19647113]

Burstein SH, McQuain CA, Ross AH, Salmonsen RA, Zurier RE, 2011 Resolution of inflammation by N-arachidonoylglycine. J. Cell. Biochem 112, 3227–3233. 10.1002/jcb.23245. [PubMed: 21732409]

Case D, Darden T, Cheatham III T, Simmerling C, Wang J, Duke R, Luo R, Walker R, Zhang W, Merz K, Roberts B, Hayik S, Roitberg A, Seabra G, Swails J, Götz A, Kolossváry I, Wong K, Paesani F, Vanicek J, Wolf R, Liu J, Wu X, Brozell S, Steinbrecher T, Gohlke H, Cai Q, Ye X, Wang J, Hsieh M, Cui G, Roe D, Mathews D, Seetin M, Salomon-Ferrer R, Sagui C, Babin V, Luchko T, Gusarov S, Kovalenko A, Kollman P, 2012 Amber 12.

Castañé A, Berrendero F, Maldonado R, 2005 The role of the cannabinoid system in nicotine addiction. Pharmacol. Biochem. Behav 81, 381–386. 10.1016/j.pbb.2005.01.025. [PubMed: 15925402]

Castañé A, Valjent E, Ledent C, Parmentier M, Maldonado R, Valverde O, 2002 Lack of CB1 cannabinoid receptors modifies nicotine behavioural responses, but not nicotine abstinence. Neuropharmacology 43, 857–867. [PubMed: 12384171]

Chaturvedi S, Driscoll WJ, Elliot BM, Faraday MM, Grunberg NE, Mueller GP, 2006 In vivo evidence that N-oleoylglycine acts independently of its conversion to oleamide. Prostag. Other Lipid Mediat 81, 136–149. 10.1016/j.prostaglandins.2006.09.001.

Chatzakos V, Slätis K, Djureinovic T, Helleday T, Hunt MC, 2012 N-acyl taurines are anti-proliferative in prostate cancer cells. Lipids 47, 355–361. 10.1007/s11745-011-3639-9. [PubMed: 22160494]

Cohen-Yeshurun A, Trembovler V, Alexandrovich A, Ryberg E, Greasley PJ, Mechoulam R, Shohami E, Leker RR, 2011 N-arachidonoyl-L-serine is neuroprotective after traumatic brain injury by reducing apoptosis. J. Cerebr. Blood Flow Metabol 31, 1768–1777. 10.1038/jcbfm.2011.53.

Cohen A, Treweek J, Edwards S, Leão RM, Schulteis G, Koob GF, George O, 2015 Extended access to nicotine leads to a CRF1 receptor dependent increase in anxiety-like behavior and hyperalgesia in rats. Addiction Biol. 20, 56–68. 10.1111/adb.12077.

De Biasi M, Dani JA, 2011 Reward, addiction, withdrawal to nicotine. Annu. Rev

Neurosci. 34, 105–130. 10.1146/annurev-neuro-061010-113734.

Devane WA, Dysarz FA, Johnson MR, Melvin LS, Howlett AC, 1988 Determination and characterization of a cannabinoid receptor in rat brain. Mol. Pharmacol 34, 605–613. [PubMed: 2848184]

Devane WA, Hanus L, Breuer A, Pertwee RG, Stevenson LA, Griffin G, Gibson D, Mandelbaum A, Etinger A, Mechoulam R, 1992 Isolation and structure of a brain constituent that binds to the cannabinoid receptor. Science 258, 1946–1949. [PubMed: 1470919]

Doll R, Peto R, Boreham J, Sutherland I, 2004 Mortality in relation to smoking: 50 years' observations on male British doctors. BMJ 328, 1519 10.1136/bmj.38142.554479.AE. [PubMed: 15213107]

Fedorova I, Hashimoto A, Fecik RA, Hedrick MP, Hanus LO, Boger DL, Rice KC, Basile AS, 2001 Behavioral evidence for the interaction of oleamide with multiple neurotransmitter systems. J. Pharmacol. Exp. Therapeut 299, 332–342.

Forget B, Coen KM, Le Foll B, 2009 Inhibition of fatty acid amide hydrolase reduces reinstatement of nicotine seeking but not break point for nicotine self-administrationd–comparison with CB1 receptor blockade. Psychopharmacology (Berl) 205, 613–624. 10.1007/s00213-009-1569-5. [PubMed: 19484221]

Forget B, Pushparaj A, Le Foll B, 2010 Granular insular cortex inactivation as a novel therapeutic strategy for nicotine addiction. Biol. Psychiatr 68, 265–271. 10.1016/j.biopsych.2010.01.029.

Gamaleddin I, Zvonok A, Makriyannis A, Goldberg SR, Le Foll B, 2012 Effects of a selective cannabinoid CB2 agonist and antagonist on intravenous nicotine self administration and reinstatement of nicotine seeking. PLoS One 7 10.1371/journal.pone.0029900 e29900. [PubMed: 22291896]

Gamaleddin IH, Trigo JM, Gueye AB, Zvonok A, Makriyannis A, Goldberg SR, Le Foll B, 2015 Role of the endogenous cannabinoid system in nicotine addiction: novel insights. Front. Psychiatr 6, 41 10.3389/fpsyt.2015.00041.

Götz AW, Williamson MJ, Xu D, Poole D, Le Grand S, Walker RC, 2012 Routine microsecond molecular dynamics simulations with AMBER on GPUs. 1. Generalized born. J. Chem. Theor. Comput 8, 1542–1555. 10.1021/ct200909j.

Hassinen T, Peräkylä M, 2001 New energy terms for reduced protein models implemented in an off-lattice force field. J. Comput. Chem 22, 1229–1242. 10.1002/jcc.1080.

Heishman SJ, Kleykamp BA, Singleton EG, 2010 Meta-analysis of the acute effects of nicotine and smoking on human performance. Psychopharmacology (Berl) 210, 453–469. 10.1007/s00213-010-1848-1. [PubMed: 20414766]

Huitron-Resendiz S, Sanchez-Alavez M, Wills DN, Cravatt BF, Henriksen SJ, 2004 Characterization of the sleep-wake patterns in mice lacking fatty acid amide hydrolase. Sleep 27, 857–865. [PubMed: 15453543]

Ignatowska-Jankowska BM, Baillie GL, Kinsey S, Crowe M, Ghosh S, Owens RA, Damaj IM, Poklis J, Wiley JL, Zanda M, Zanato C, Greig IR, Lichtman AH, Ross RA, 2015 A cannabinoid CB1

receptor-positive allosteric modulator reduces neuropathic pain in the mouse with No psychoactive effects. Neuropsychopharmacology 40, 2948–2959. 10.1038/npp.2015.148. [PubMed: 26052038]

Ignatowska-Jankowska BM, Muldoon PP, Lichtman AH, Damaj MI, 2013 The cannabinoid CB2 receptor is necessary for nicotine-conditioned place preference, but not other behavioral effects of nicotine in mice. Psychopharmacology (Berl) 229, 591–601. 10.1007/s00213-013-3117-6. [PubMed: 23652588]

Jackson A, Bagdas D, Muldoon PP, Lichtman AH, Carroll FI, Greenwald M, Miles MF, Damaj MI, 2017 In vivo interactions between α7 nicotinic acetylcholine receptor and nuclear peroxisome proliferator-activated receptor-α: implication for nicotine dependence. Neuropharmacology 118, 38–45. 10.1016/j.neuropharm.2017.03.005. [PubMed: 28279662]

Jackson KJ, Kota DH, Martin BR, Damaj MI, 2009 The role of various nicotinic receptor subunits and factors influencing nicotine conditioned place aversion. Neuropharmacology 56, 970–974. 10.1016/j.neuropharm.2009.01.023. [PubMed: 19371584]

Jackson KJ, Martin BR, Changeux JP, Damaj MI, 2008 Differential role of nicotinic acetylcholine receptor subunits in physical and affective nicotine withdrawal signs. J. Pharmacol. Exp. Therapeut 325, 302–312. 10.1124/jpet.107.132977.

Justinova Z, Panlilio LV, Moreno-Sanz G, Redhi GH, Auber A, Secci ME, Mascia P, Bandiera T, Armirotti A, Bertorelli R, Chefer SI, Barnes C, Yasar S, Piomelli D, Goldberg SR, 2015 Effects of fatty acid amide hydrolase (FAAH) inhibitors in non-human primate models of nicotine reward and relapse. Neuropsychopharmacology 40, 2185–2197. 10.1038/npp.2015.62. [PubMed: 25754762]

Kota D, Martin BR, Robinson SE, Damaj MI, 2007 Nicotine dependence and reward differ between adolescent and adult male mice. J. Pharmacol. Exp. Therapeut 322, 399–407. 10.1124/jpet.107.121616.

Kutlu MG, Burke D, Slade S, Hall BJ, Rose JE, Levin ED, 2013 Role of insular cortex D1 and D2 dopamine receptors in nicotine self-administration in rats. Behav. Brain Res 256, 273–278. 10.1016/j.bbr.2013.08.005. [PubMed: 23948214]

Le Foll B, Goldberg SR, 2004 Rimonabant, a CB1 antagonist, blocks nicotine-conditioned place preferences. Neuroreport 15, 2139–2143. [PubMed: 15486497]

Little PJ, Compton DR, Johnson MR, Melvin LS, Martin BR, 1988 Pharmacology and stereoselectivity of structurally novel cannabinoids in mice. J. Pharmacol. Exp. Therapeut 247, 1046–1051.

Martin BR, Compton DR, Thomas BF, Prescott WR, Little PJ, Razdan RK, Johnson MR, Melvin LS, Mechoulam R, Ward SJ, 1991 Behavioral, biochemical, and molecular modeling evaluations of cannabinoid analogs. Pharmacol. Biochem. Behav 40, 471–478. [PubMed: 1666911]

Mascia P, Pistis M, Justinova Z, Panlilio LV, Luchicchi A, Lecca S, Scherma M, Fratta W, Fadda P, Barnes C, Redhi GH, Yasar S, Le Foll B, Tanda G, Piomelli D, Goldberg SR, 2011 Blockade of nicotine reward and reinstatement by activation of alpha-type peroxisome proliferator-activated receptors. Biol. Psychiatr 69, 633–641. 10.1016/j.biopsych.2010.07.009.

Mechoulam R, Ben-Shabat S, Hanus L, Ligumsky M, Kaminski NE, Schatz AR, Gopher A, Almog S, Martin BR, Compton DR, Pertwee RG, Griffin G, Bayewitch M, Barg J, Vogel Z, 1995 Identification of an endogenous 2-monoglyceride, present in canine gut, that binds to cannabinoid receptors. Biochem. Pharmacol 50, 83–90. 10.1016/0006-2952(95)00109-D. [PubMed: 7605349]

Melis M, Pistis M, 2014 Targeting the interaction between fatty acid ethanolamides and nicotinic receptors: therapeutic perspectives. Pharmacol. Res 86, 42–49. 10.1016/j.phrs.2014.03.009. [PubMed: 24704146]

Melis M, Scheggi S, Carta G, Madeddu C, Lecca S, Luchicchi A, Cadeddu F, Frau R, Fattore L, Fadda P, Ennas MG, Castelli MP, Fratta W, Schilstrom B, Banni S, De Montis MG, Pistis M, 2013 PPARα regulates cholinergic-driven activity of midbrain dopamine neurons via a novel mechanism involving α7 nicotinic acetylcholine receptors. J. Neurosci 33, 6203–6211. 10.1523/JNEUROSCI.4647-12.2013. [PubMed: 23554501]

Merritt LL, Martin BR, Walters C, Lichtman AH, Damaj MI, 2008 The endogenous cannabinoid system modulates nicotine reward and dependence. J. Pharmacol. Exp. Therapeut 326, 483–492. 10.1124/jpet.108.138321.

Morris GM, Huey R, Lindstrom W, Sanner MF, Belew RK, Goodsell DS, Olson AJ, 2009 AutoDock4 and AutoDockTools4: automated docking with selective receptor flexibility. J. Comput. Chem 30, 2785–2791. 10.1002/jcc.21256. [PubMed: 19399780]

Naqvi NH, Bechara A, 2010 The insula and drug addiction: an interoceptive view of pleasure, urges, and decision-making. Brain Struct. Funct 214, 435–450. 10.1007/s00429-010-0268-7. [PubMed: 20512364]

Naqvi NH, Gaznick N, Tranel D, Bechara A, 2014 The insula: a critical neural substrate for craving and drug seeking under conflict and risk. Ann. N. Y. Acad. Sci 1316, 53–70. 10.1111/nyas.12415. [PubMed: 24690001]

Naqvi NH, Rudrauf D, Damasio H, Bechara A, 2007 Damage to the insula disrupts addiction to cigarette smoking. Science 315, 531–534. 10.1126/science.1135926. [PubMed: 17255515]

Navarrete F, Rodríguez-Arias M, Martín-García E, Navarro D, García-Gutiérrez MS, Aguilar MA, Aracil-Fernández A, Berbel P, Miñarro J, Maldonado R, Manzanares J, 2013 Role of CB2 cannabinoid receptors in the rewarding, reinforcing, and physical effects of nicotine. Neuropsychopharmacology 38, 2515–2524. 10.1038/npp.2013.157. [PubMed: 23817165]

Ortar G, Cascio MG, De Petrocellis L, Morera E, Rossi F, Schiano-Moriello A, Nalli M, de Novellis V, Woodward DF, Maione S, Di Marzo V, 2007 New N-arachidonoylserotonin analogues with potential “dual” mechanism of action against pain. J. Med. Chem 50, 6554–6569. 10.1021/jm070678q. [PubMed: 18027904]

Panlilio LV, Justinova Z, Mascia P, Pistis M, Luchicchi A, Lecca S, Barnes C, Redhi GH, Adair J, Heishman SJ, Yasar S, Aliczki M, Haller J, Goldberg SR, 2012 Novel use of a lipid-lowering fibrate medication to prevent nicotine reward and relapse: preclinical findings. Neuropsychopharmacology 37, 1838–1847. 10.1038/npp.2012.31. [PubMed: 22453137]

Perkins KA, Karelitz JL, Michael VC, Fromuth M, Conklin CA, Chengappa KNR, Hope C, Lerman C, 2016 Initial evaluation of fenofibrate for efficacy in aiding smoking abstinence. Nicotine Tob. Res 18, 74–78. 10.1093/ntr/ntv085. [PubMed: 25895948]

Piscitelli F, Carta G, Bisogno T, Murru E, Cordeddu L, Berge K, Tandy S, Cohn JS, Griinari M, Banni S, Di Marzo V, 2011 Effect of dietary krill oil supplementation on the endocannabinoidome of metabolically relevant tissues from high-fat-fed mice. Nutr. Metab. (Lond) 8, 51 10.1186/1743-7075-8-51. [PubMed: 21749725]

Pushparaj A, Hamani C, Yu W, Shin DS, Kang B, Nobrega JN, Le Foll B, 2013 Electrical stimulation of the insular region attenuates nicotine-taking and nicotine-seeking behaviors. Neuropsychopharmacology 38, 690–698. 10.1038/npp.2012.235. [PubMed: 23249816]

Pushparaj A, Kim AS, Musiol M, Trigo JM, Le Foll B, 2015 Involvement of the rostral agranular insular cortex in nicotine self-administration in rats. Behav. Brain Res 290, 77–83. 10.1016/j.bbr.2015.04.039. [PubMed: 25934486]

Robinson JD, Cinciripini PM, Karam-Hage M, Aubin H-J, Dale LC, Niaura R, Anthenelli RM, STRATUS Group, 2017 Pooled analysis of three randomized, double-blind, placebo controlled trials with rimonabant for smoking cessation. Addiction Biol. 10.1111/adb.12508.

Ryckaert J-P, Ciccotti G, Berendsen HJ, 1977 Numerical integration of the cartesian equations of motion of a system with constraints: molecular dynamics of n-alkanes. J. Comput. Phys 23, 327–341. 10.1016/0021-9991(77)90098-5.

Scheggi S, Melis M, De Felice M, Aroni S, Muntoni AL, Pelliccia T, Gambarana C, De Montis MG, Pistis M, 2016 PPARa modulation of mesolimbic dopamine transmission rescues depression-related behaviors. Neuro-pharmacology 110, 251–259. 10.1016/j.neuropharm.2016.07.024.

Simonnet A, Cador M, Caille S, 2013 Nicotine reinforcement is reduced by cannabinoid CB1 receptor blockade in the ventral tegmental area. Addiction Biol. 18, 930–936. 10.1111/j.1369-1600.2012.00476.x.

Sugiura T, Kondo S, Sukagawa A, Nakane S, Shinoda A, Itoh K, Yamashita A, Waku K, 1995 2-Arachidonoylgylcerol: a possible endogenous cannabinoid receptor ligand in brain. Biochem. Biophys. Res. Commun 215, 89–97. 10.1006/bbrc.1995.2437. [PubMed: 7575630]

Valjent E, Mitchell JM, Besson M-J, Caboche J, Maldonado R, 2002 Behavioural and biochemical evidence for interactions between Δ9-tetrahydrocannabinol and nicotine. Br. J. Pharmacol 135, 564–578. 10.1038/sj.bjp.0704479. [PubMed: 11815392]

Wang J, Wolf RM, Caldwell JW, Kollman PA, Case DA, 2004 Development and testing of a general amber force field. J. Comput. Chem 25, 1157–1174. 10.1002/jcc.20035. [PubMed: 15116359]

Wang S, Xu Q, Shu G, Wang L, Gao P, Xi Q, Zhang Y, Jiang Q, Zhu X, 2015 NOleoyl glycine, a lipoamino acid, stimulates adipogenesis associated with activation of CB1 receptor and Akt signaling pathway in 3T3-L1 adipocyte. Biochem. Biophys. Res. Commun 466, 438–443. 10.1016/j.bbrc.2015.09.046. [PubMed: 26365347]

Watkins SS, Koob GF, Markou A, 2000 Neural mechanisms underlying nicotine addiction: acute positive reinforcement and withdrawal. Nicotine Tob. Res 2, 19–37. [PubMed: 11072438]

Wiley JL, Martin BR, 2003 Cannabinoid pharmacological properties common to other centrally acting drugs. Eur. J. Pharmacol 471, 185–193. 10.1016/S0014-2999(03)01856-9. [PubMed: 12826237]

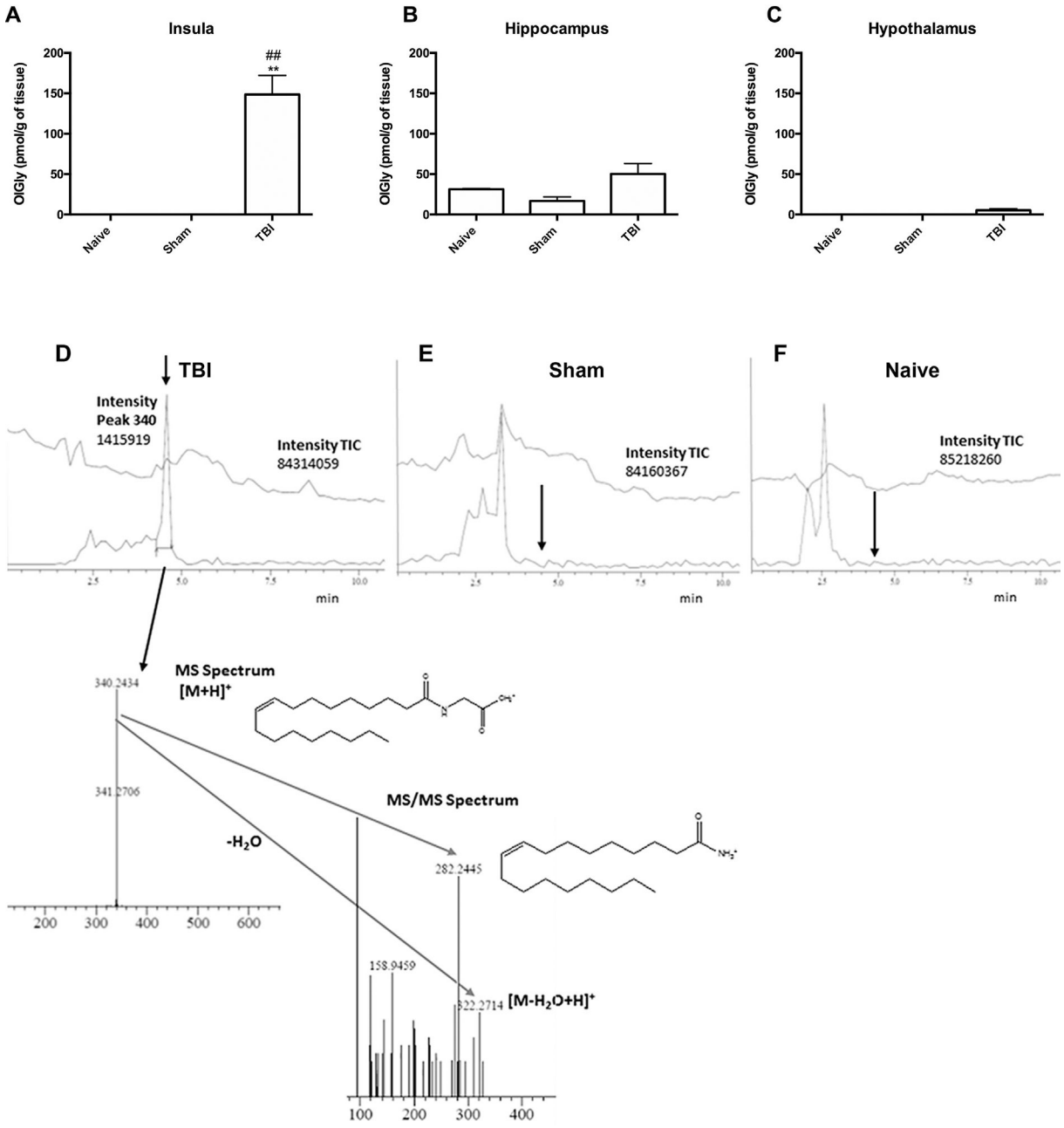

Fig. 1.

Traumatic brain injury (TBI) leads to increased OlGly levels in the insular cortex of mice. (**A**) Mice subjected to TBI display significant increases of OlGly in the insula, but not in (**B**) hippocampus or (**C**) hypothalamus. Values represent the mean ± SEM of n = 5. **p < 0.001 vs naïve; ##p < 0.001 vs sham. (**D**) A representative chromatogram shows the presence of OlGly in the insula of mice 24 h following TBI. Injured insula shows formation of OlGly as confirmed by MS and MS/MS spectra. However, OlGly was below the limit of detection in sham (**E**) and naïve mice (**F**). The arrow depicts the retention time of OlGly from the standard. The upper chromatogram traces represent the total ion current (TIC), and lower chromatogram traces represent the extracted chromatograms *m/z* around 340 amu in (**D-F**).

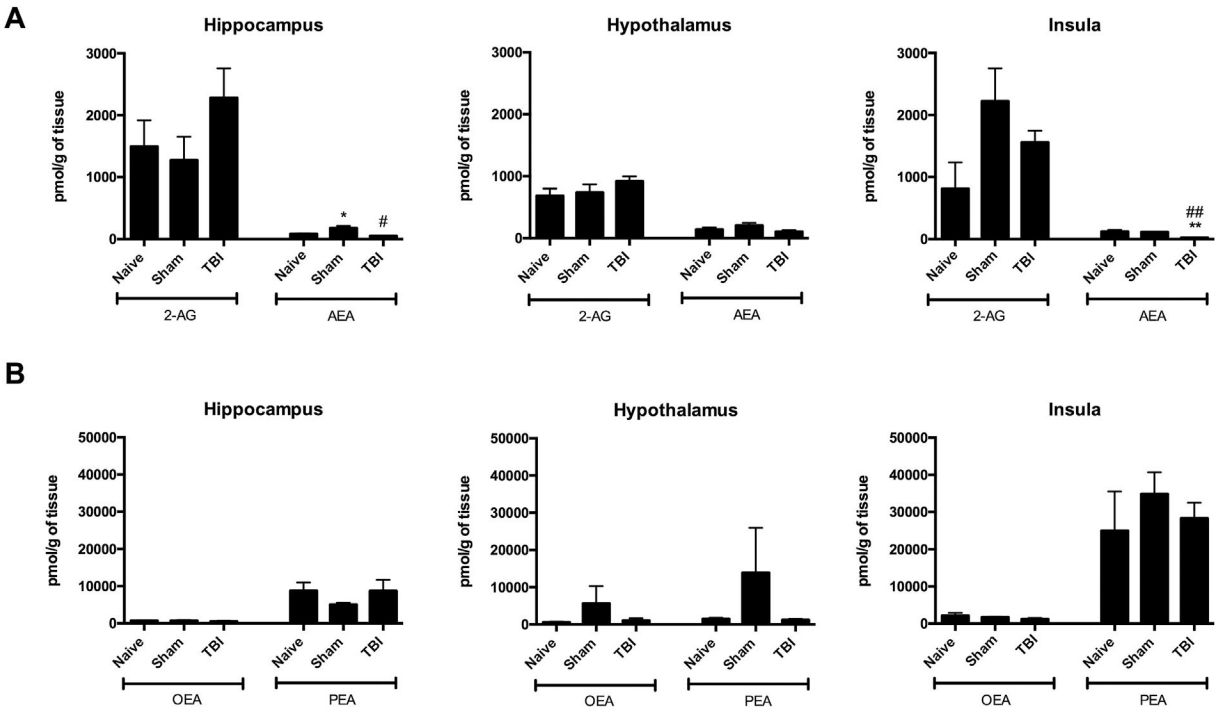

Fig. 2.

Levels of endocannabinoids in the hippocampus, hypothalamus and insula of sham mice and mice following weight drop-induced traumatic brain injury. (**A**) Levels of anandamide (AEA) and 2-arachidonoylglycerol (2-AG). (**B**) Palmitoylethanolamide (PEA) and oleoylethanolamide (OEA) levels. Values represent means ± SEM of n = 4–5 experiments. **p 0.001, *p < 0.05 vs naïve; ##p < 0.001, #p < 0.05 vs sham.

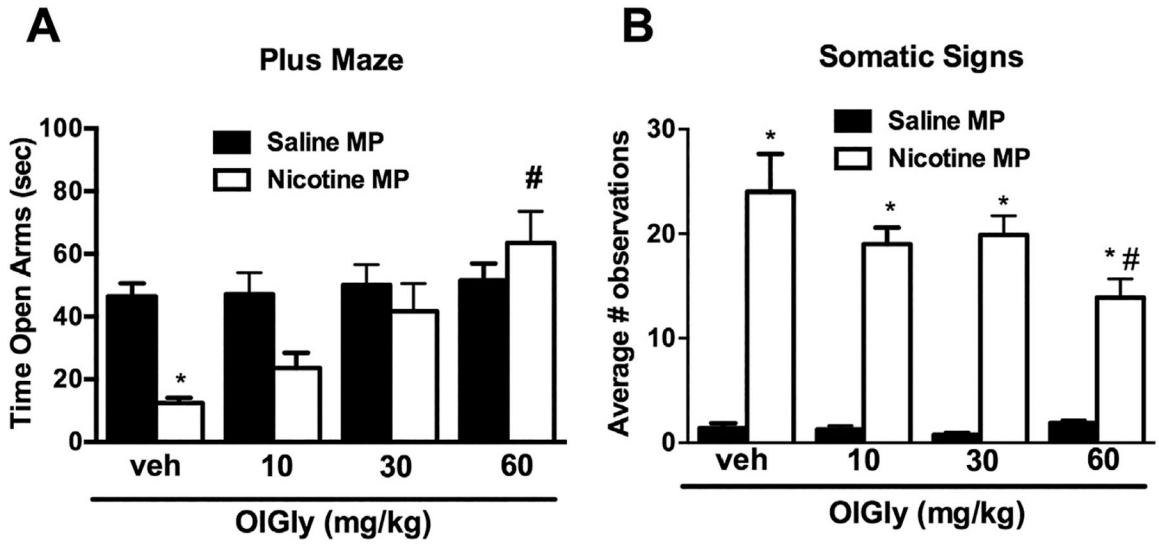

Fig. 3.

OlGly prevents mecamylamine-precipitated withdrawal signs in nicotine-dependent mice. Intraperitoneal administration of OlGly significantly (**A**) increased time spent in the open arms of the elevated plus maze compared to nicotine-pelleted mice that were given an injection of vehicle, and (B) decreased total somatic signs. All mice were challenged with mecamylamine (2 mg/kg, s.c.) prior to testing. MP: minipump. Values represent the mean ± SEM of n = 7–8 mice per group. *$p < 0.05$ vs. saline/vehicle; #$p < 0.05$ vs. nicotine/vehicle.

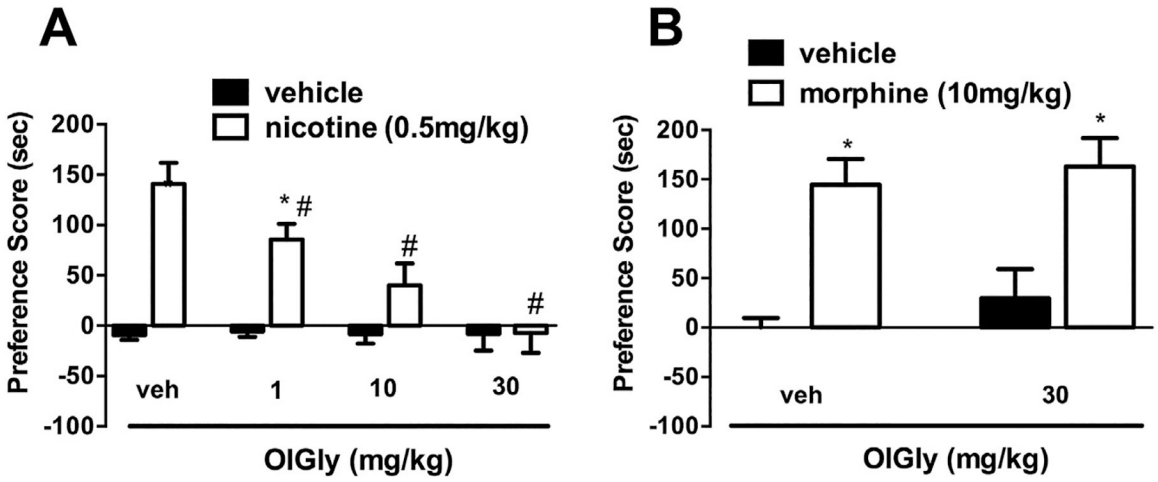

Fig. 4.

OlGly prevents nicotine reward, but not morphine reward. (**A**) OlGly dose-dependently blocked nicotine CPP, (**B**) but did not attenuate morphine (30 mg/kg, i.p.) CPP. Values represent the mean ± SEM of n = 7–8 mice per group. *p < 0.05 vs. saline/vehicle; #p < 0.05 vs. nicotine/vehicle.

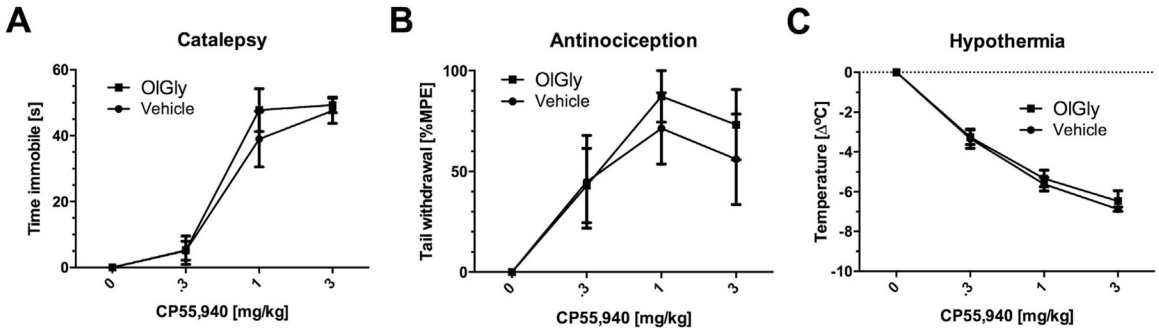

Fig. 5.

OlGly does not act as a CB_1 receptor allosteric modulator in the *in vivo* triad assay. CP55,940 (0, 0.3, 1, and 3 mg/kg) dose-dependently induced (**A**) catalepsy, (**B**) antinociception, and (**C**) hypothermia in vehicle-pretreated mice. Pretreatment with OlGly (60 mg/kg) did not induce any changes in the dose-response curve of CP55,940 for any of these dependent measures. Values represent means ± SEM of n = 5/6 mice per group.

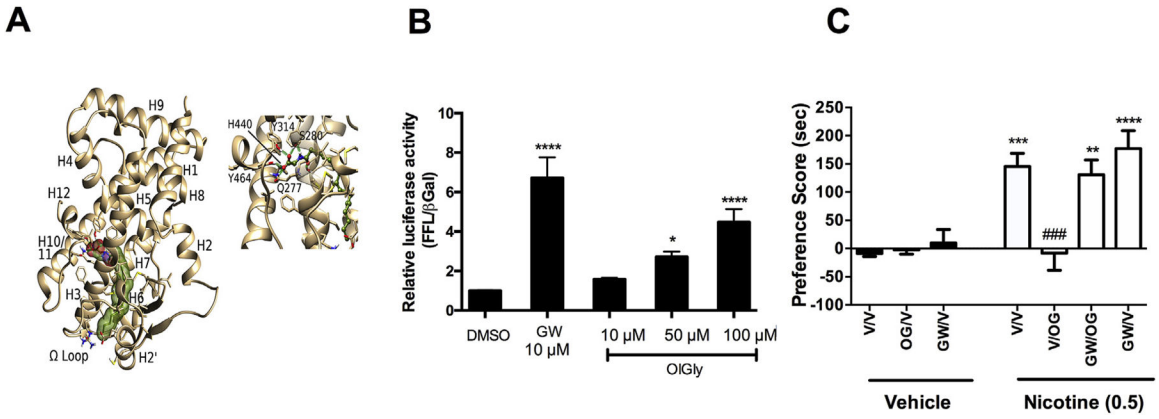

Fig. 6.

PPAR-α mediates the anti-reward effects of OlGly. (**A**) Representative frame from MD of OlGly/PPAR-α complex and details of ligand-protein interactions in the ligand binding site. The carboxylic moiety of the ligand recapitulates the main polar stabilizing interactions with Tyr464(H12), Tyr314(H5), His440(H10/11) and Ser280(H3), signature of a PPAR-α agonist. (**B**) Luciferase Assay for PPAR-α/RXR. Relative Luciferase Units in response to OlGly and the PPAR-α agonist GW7647 (comparison drug). DMSO (n = 12), GW7647 (GW) 10 mM (n = 6), OlGly 10 mM (n = 7), 50 μM (n = 9) and 100 mM (n = 11). ****p < 0.0001, *p < 0.05 vs DMSO (**C**) The selective PPAR-α antagonist GW6471 (2 mg/kg) prevented OlGly-induced inhibition of nicotine CPP. n = 6–8 mice per group. ****p < 0.0001. ***p < 0.001, **p < 0.01 vs. vehicle/vehicle; ###p < 0.001 vs. nicotine/vehicle. Values represent the mean ± SEM.

Table 1

OlGly does not elicit *in vivo* pharmacological effects as assessed in the tetrad assay. OlGly did not produce catalepsy, antinociception, hypothermia, or motor behavior, as reflected by the following measures: distance traveled, speed, and immobility time. Values represent means ± SEM of n = 9 mice per group.

Treatment	Catalepsy (s)	Antinociception (%MPE)	Δ rectal temperature (°C)	Distance traveled (cm)	Speed (cm/s)	Time immobile (s)
vehicle	0.0	6.0 ± 5.1	−0.41 ± 0.30	20.8 ± 2.3	6.9 ± 0.8	7.1 ± 1.5
OlGly 10 mg/kg	0.0	12.0± 6.6	−0.90 ± 0.19	24.3 ±1.2	8.1 ± 0.4	8.6 ± 1.6
OlGly 30 mg/kg	0.0	6.0 ± 4.5	−1.13 ± 0.26	21.5±1.7	7.2 ± 0.6	11.8 ±6.2
OlGly 100 mg/kg	0.0	25.9±11.0	−0.22 ± 0.5431	18.6±1.5	6.21 ±0.5	17.4 ± 7.3

Table 2

OlGly does not functionally interact with the endogenous cannabinoid system. OlGly shows low affinity for CB_1 and CB_2 receptors and has very low potency in inhibiting FAAH. Values represent mean ± SEM (n = 3), % displacement or inhibition, n = 2.

CB_1 IC_{50} (μM)	**CB_1 Ki (μM)**	**CB_1 displacement produced by maximum dose tested (50 μM)**	**CB_2 IC_{50} (μM)**	**CB_2 Ki (μM)**	**CB_2 displacement produced by maximum dose tested (50 μM)**	**IC_{50} FAAH inhibition (μM)**	**FAAH inhibition produced by maximum dose tested (50 μM)**
45.5 ± 5.1	27.8 ± 3.1	55.9 ± 7.3%	>50	>50	15.5 ± 6.40%	8.65	89.4%